Available online at www.sciencedirect.com

SciVerse ScienceDirect

Ceramics International 38 (2012) 5333–5340

CERAMICS INTERNATIONAL

www.elsevier.com/locate/ceramint

Synthesis and characterization of bioactive zirconia toughened alumina doped with HAp and fluoride compounds

Vinay Kumar Singh *, B. Ravindra Reddy

Department of Ceramic Engineering, Institute of Technology, Banaras Hindu University, Varanasi 221005, India

Received 18 January 2012; received in revised form 14 March 2012; accepted 14 March 2012
Available online 30 March 2012

Abstract

Alumina–zirconia nanostructured composites (ZrO_2 addition by 20 wt%) were prepared using combined gelation–precipitation process. A modified sol–gel process has been developed to prepare nano structured spinel [$MgAl_2O_4$], Al_2O_3, ZrO_2 and their composite materials. This process is useful in retaining tetragonal phase of zirconia at room temperature, which provides transformation toughening in the nano composites. Dried gels powders were calcined up to 1250 °C. Similarly, hydroxyapatite powders were produced by wet-chemical method and calcined at different temperatures. All the dried gel and calcined powders were characterized by using X-ray diffraction, DTA/TGA and SEM. Samples were prepared by uniaxial pressing the composites powders using ZTA, HAp, MgF_2 and CaF_2 in different ratio. Incorporation of CaF_2 and MgF_2 as a source for fluorine was also done to improve the sinterability of composites. The samples were sintered at 1400 °C for three hours. Densification and mechanical behaviour of sintered samples were observed. Bioactivities of all compositions were tested using SBF solution and then characterizing by FTIR. The main objective of work was to dope ZTA nano composites with HAp and fluoride compounds to obtain better sinterability at lower temperatures. Then evaluate the obtained ZTA based bioactive composite ceramics that have high mechanical strengths. This study verifies the bioactivities of HAp-added ZTA composites.

Keywords: A. Sintering; B. Nanocomposites; C. Mechanical properties; D. Apatite; E. Biomedical applications

1. Introduction

Alumina and zirconia are well known mechanically compatible bio ceramic materials, possessing high strength, wear resistance and hardness [1–6]. These properties make them along with their combination, known as zirconia toughened alumina [ZTA], to be used in dentistry and orthopedic situations such as hip and knee joints. However, these ceramics are bio inert material and they do not directly bond with natural bone in many replacements [7–12]. On the other hand, hydroxyapatite [(HAp,$Ca_{10}(PO4)_6(OH)_2$)] ceramics similar to the calcified tissues of vertebrates are used as implant biomaterials, because HAp bonds to bone directly and promotes the new bone formation necessary for osseointegration implant [8–12]. Due to poor mechanical properties, HAp bioactive ceramics cannot be the substitutive materials for load-bearing parts. Therefore, mechanical properties of HAp have to be improved for such applications [13–17]. There are two possible ways by which this material can be applied and researches are being carried out in these areas. Among them, one method is to apply bioactive materials as a coating on the bio inert materials such as metallic and ceramic implants, while the other approach is to make composites of bioactive and inert materials. Metallic implants coated with HAp, are generally used as load-bearing implants, but susceptibility of the HAp coating to debond from the metallic substrate has limited its uses [18].

The second approach can be subdivided into two distinct strategies depending on whether HAp as a major part of the composites or HAp doped composites can be used. The reinforcement of HA, which is accomplished by the addition of other materials in the form of powders, platelets, or fibers, belongs to the first one. As lower strength and fracture toughness of the HAp ceramics have limited its applications in biomedical implants [19] to certain circumstances, therefore,

* Corresponding author. Tel.: +91 0542 6701870/+91 9936182124; fax: +91 0542 2369162.
E-mail address: vinaycer@gmail.com (V.K. Singh).

0272-8842/$36.00
doi:10.1016/j.ceramint.2012.03.039

ZrO_2 or Al_2O_3 added HAp composites with high mechanical properties and bioactivity is to be developed [20,21]. To enhance the strength of the HAp ceramic, HAp-based composites ceramics, such as ZrO_2 doped HA composites, have been studied. These composites do not have high strength and fracture toughness, because the added ZrO_2 prevented densification of the HAp [22,23]. In studies involving the use of these materials, the mechanical properties of the HAp-based composites were found to be enhanced nearly by three times [24,25]. However, further improvements are needed before such materials can be employed for load-bearing applications such as dental/orthopedic implants. Therefore second strategy will be beneficial by involving the improvement of the biocompatibility of various strong materials through the incorporation of bioactive materials. The zirconia–alumina system (ZTA, 80 wt% ZrO_2–20 wt% Al_2O_3) is well-known for its high flexural strength, and is classified as a bio inert ceramic [26]. Therefore, ZTA is considered to be one of the most suitable materials to be used as a matrix for the HAp-added strong composites.

Therefore, our objective was to dope the small amount of HAp and evaluate the obtained ZTA based bioactive composite ceramic that has a high strength and fracture toughness. In this context, the current study focused on developing the bioactivity of strong ZTA nano-composites doped with HAp. This study verifies the bioactivities of HAp-added ZTA composites. Incorporation of CaF_2 and MgF_2 as a source for fluorine was also done to improve the sinterability of composites [27–33]. alumina–zirconia nanostructured composites (ZrO_2 addition by 20 wt%) were prepared using combined gelation–precipitation process as reported earlier [34–41]. A modified sol–gel process has been developed to prepare nano structured spinel [$MgAl_2O_4$], Al_2O_3, ZrO_2 and their composite materials. This process is useful in retaining tetragonal phase of zirconia at room temperature, which provides transformation toughening in the nano composites [38–41]. Dried gels powders were calcined up to 1250 °C. Similarly, hydroxyapatite powders were produced by wet-chemical method [42] and calcined at different temperatures. All the dried gel and calcined powders were characterized by using X-ray diffraction, DTA/TGA and SEM. Samples were prepared by uniaxial pressing the composites powders using ZTA, HAp, MgF_2 and CaF_2 in different ratio. The samples were sintered at 1400 °C for three hours. Densification and mechanical behaviour of sintered samples were observed. Bioactivities of all compositions were tested using SBF solution and then characterizing by FTIR [43–46].

2. Experimental

2.1. Preparation of nano composite powders

The alumina–zirconia (adding ZrO_2 by 20 wt%) nano composites were prepared by combined gelation and precipitation process. Starting materials were analytical grade reagents of $Al_2(SO_4)_3{\cdot}16H_2O$ and zirconium oxychloride $ZrOCl_2{\cdot}8H_2O$. The concentration of the starting solutions of aluminium sulphate and zirconium oxychloride was kept 0.50 mol/liter. In this process, the concentration of the starting solutions is taken high to such an extent that during the gelation process, when the gel becomes fully viscous, a substantial amount of starting solute remains within the gel network. When the gel is dried, the solutes are precipitated out of the gel network in the pores between hydroxide particles with size of the same order. The gel is therefore a combination of precipitated solute and gel particles. These composite gels are colloidal in nature. Calcination of gel at a suitable temperature will give powders from the decomposition of these two sources. Details of synthesis of nanocrystalline zirconia–alumina composites powders, their particle size distribution, characterization, and sintering behaviour have been reported previously [34–41]. The tetragonal phase in ZTA is retained nearly 80% in calcined powders as calculated by Garvie's equation [40]. Gels of composites were dried and then calcined at 1200 °C for three hours. Heating rate was kept at 10 °C/min. DTA/TGA analysis of dried gel powders was done and XRD patterns were taken of dried gel and of calcined powders.

Similarly, hydroxyapatite powder was produced by solution–precipitation method [42]. Analytical reagent grade of chemicals such as calcium nitrate [$Ca(NO_3)_2{\cdot}4H_2O$], magnesium chloride [$MgCl_2{\cdot}6H_2O$], sodium hydrogen carbonate [$NaHCO_3$], sodium hydroxide [NaOH], ammonium di-hydrogen phosphate [$NH_4H_2PO_4$] were used. For maintining the pH of the solution during precipitation, ammonia solution was used as agents for pH adjustment. Solution of 0.24 M $Ca(NO_3)_2{\cdot}4H_2O$ first prepared using double distilled water. It was vigorously stirred and no working temperature was maintained. All the reactions were done at room temperature (~27 °C). A prepared solution of 0.29 M $(NH_4)_2HPO_4$ was slowly added dropwise to the $Ca(NO_3)_2{\cdot}4H_2O$ solution with simultaneously stirring. The ratio of Ca/P was kept about 1.64. The precipitates were filtered and dried at 80 °C in an electric oven. Dried HAp gel powders were ground in planetary ball mill using tungsten carbide as grinding media for 30 min and then sieved through 44 μm sieves by using programmable sieve shaker. The ground powders were calcined at 1200 °C for one hour. The dried gel powders as well as calcined HAp powders were characterized by X-ray diffraction, DTA/TGA, and scanning electron microscopy.

2.2. Preparation of composites and their mechanical behaviour

Various mixes were prepared by mixing prepared ZTA and HAp powders. Magnesium fluoride, calcium fluoride and PVA solution were also incorporated in the batches according to the compositions as given in Table 1. The first composition to study was pure ZTA composite without any addition. This composition was selected for comparative purpose. It will help to observe how the physical properties are being changed on introduction of HAp and fluoride compounds in it. Batches were mixed in planetary ball mill in dry state with tungsten carbide coated steel balls and jar as grinding media. The powder mixtures were pressed uniaxially in steel molds at room

Table 1
Compositions of HAp and fluoride mixed ZTA composites.

Materials	Composition 1	Composition 2	Composition 3	Composition 4	Composition 5
ZTA	100 parts	100 parts	100parts	100 parts	100 parts
HAp	–	10 parts	20 parts	30 parts	40 parts
MgF_2	–	3 parts	3 parts	3 parts	3 parts
CaF_2	–	3 parts	3 parts	3 parts	3 parts

temperature with an applied pressure of 80 kg/cm^2. The diameter of pellets was 1.5 cm and of dimensions of cubes were 1cubic inch. Rectangular bars of 25 mm × 15 mm × 10 mm were also prepared using the sample pressure value. The prepared samples were sintered isothermally at 1400 °C for three hours. Heating rate was 10 °C/min. Bulk densities of sintered pellets were measured by water displacement method. Table 2 shows bulk density and mechanical properties of all compositions at the sintering temperature of 1400 °C.

All bars were fractured in a three point bending fixture with an outer span of 20 mm. Polished and indented surfaces were subjected to tensile stress generated by UTM machine (Shimandzu, Japan). Crosshead speed was maintained at 0.05 mm min. A load–deflection plot was recorded. All the samples were fractured in the above manner and the fracture load was noted. One blank run was made on the fixture without sample and a load–strain curve was used to correct all other plots for stiffness of the loading system. Compressive strengths of the cubic bars were also measured. All the samples were compressed and fractured in the above manner and the final compressive load was noted. At least five specimens were tested for both the compressive strength and the bending strength measurements and the strength data were reported as the average value [47–49]. The bending strength was finally calculated based on the following equation [50]:

$$\sigma = \frac{3PL}{2bd^2} \quad (1)$$

where σ denotes the bending strength, P denotes the applied maximum load, and L, b and d are the span length, the width and the thickness of the test specimen, respectively.

The compressive strength, C (MPa), was calculated using the following equation [48]:

$$C = \frac{P}{L^2} \quad (2)$$

where P is the maximum applied load (N) and L is the side of the cubic sample.

The phase determination in sintered samples was done by X-ray diffractometer (Žusing Philips, 1710 X-ray powder diffract meter, 40 kV/20 mA and Fe-filtered Cu Kα radiation of wavelength 1.79 Å). The sintered samples were polished using diamond paste and then thermally etched at 1200 °C for observation under SEM.

2.3. In vitro bioactivity in samples

To study bioactivity of HAp and fluoride doped ZTA composites, sintered samples were immersed in SBF solution. SBF solution was prepared as described in various research papers [51–53]. In vitro bioactivity test was carried out on the dried sintered pellets of all compositions. Analytically reagent grade NaCl, $NaHCO_3$, KCl, $K_2HPO_4{\cdot}3H_2O$, $MgCl_2{\cdot}6H_2O$, $CaCl_2$ and Na_2SO_4 were dissolved in ion exchanged water and the resulting solution has an aqueous solution consisting of Ca^{2+}: 2.5 mM, Na^+: 142.0 mM, Mg^{2+}: 1.5 mM, K^+: 5.0 mM, Cl^-: 103.0 mM, HCO^{3-}: 27.0 mM, $HPO_4{}^-$: 1.0 mM and SO: 0.5 mM. The solution was buffered at a pH of 7.4 with (tris-hydroxymethyl)-aminomethane and hydrochloric acid. The temperature of the solution was maintained at 37 °C (±1 °C) throughout the experiment to simulate a human physiological environment. A 50 ml amount of SBF solution, having pH 7.2, was taken in each air tight plastic jar. Sintered pellets were kept individually in SBF solution containing jar and all containers were kept in an incubator at static condition with maintaining 37.8 °C. Samples, immersed in SBF, were taken out after 3, 7, 15 and 30 days. The samples were gently rinsed in ion exchanged water. After that, these samples were dried and stored in desiccators. The surface of the samples, treated in SBF, were analyzed using Fourier transform infrared spectrometer (FTIR), IS10 Nicolet, USA); since bioactivity is determined by the formation of calcium phosphate layer on the surface of the samples.

Table 2
Densification and mechanical data of HAp and fluoride doped ZTA composites.

Composition no.	Bulk density (g/cm^3)	Compressive strength (MPa)	Bending strength (MPa)
1	3.52	470	296
2	3.60	496	314
3	3.73	505	347
4	3.80	522	362
5	3.84	543	387

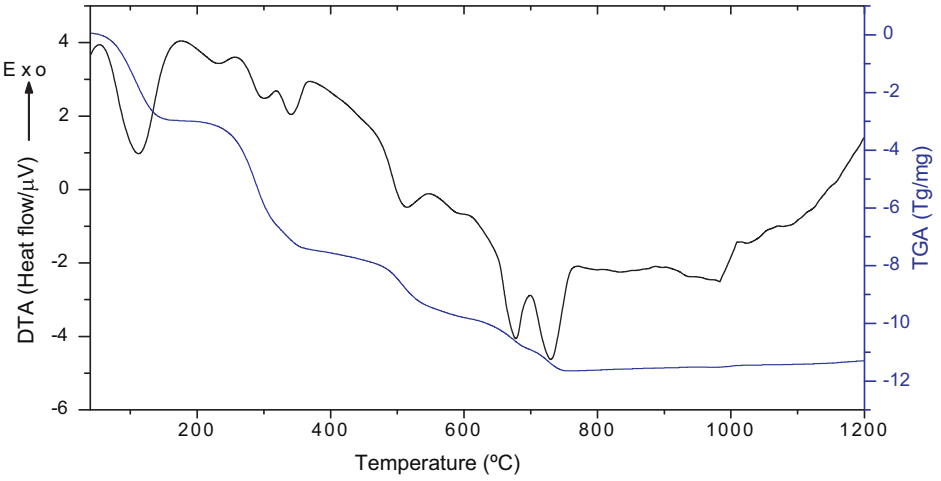

Fig. 1. DTA/TGA of HAp gel powder prepared by solution–precipitation method.

3. Results and discussion

3.1. Synthesis and characterization of fluoride doped ZTA-HAp composites

Syntheses of nanocrystalline zirconia–alumina composites powders, prepared by combined gelation–precipitation process, have been reported earlier [34–41]. It was observed that calcined powders as well as sintered samples of ZTA (up to 20 wt% ZrO_2) have more fraction of t-ZrO_2 in alumina matrix. The tetragonal phase in ZTA is retained up to 80% of total zirconia. Characterization results on composite powders of alumina containing various amount of zirconia showed that alumina was present in α-phase in all compositions. Calcined powders have particle sizes in the range of 100–300 nm and observations on microstructure of sintered samples showed that alumina matrix has 200–300 nm average grain size and zirconia grains have 200 nm average sizes with uniform distribution in alumina matrix in all cases. Good initial sinterability of all powders was evident. Theoretical densities of all compositions were calculated on the assumption that zirconia was present in tetragonal phase and alumina as α-Al_2O_3. More than 80% of the theoretical densities were observed in all compositions when samples sintered isothermally at 1400 °C for three hours and slow densification was noticeable in Al_2O_3 samples by increasing ZrO_2 content. Hydroxyapatite powder was produced by solution–precipitation method. The DTA/TGA of HAp gel powder is shown in Fig. 1. Three exothermic peaks are clearly observed around 190 °C, 280 °C and 380 °C. Six endothermic peaks around 100 °C, 310 °C, 480 °C, 680 °C, 740 °C and 995 °C are also observed in DTA analysis. The endothermic peaks at lower temperatures are due to loss of free water and removal of hydroxyl ions. It is also supported by the sharp weight loss shown in the TGA graph. The endothermic peaks in intermediate temperature are for the decomposition of ammonium salts remained in the gel. The exothermic peaks may be due to initial decomposition of calcium carbonate phase with corresponding weight loss in TGA curve. Another endothermic peak around 1000 °C can be attributed to the conversion of HAp into crystalline calcium phosphate. From the XRD data as shown in Fig. 2 of the calcined HAp gel powders, major peaks are matched with calcium phosphate phase ($Ca_4P_2O_9$); JCPDS file No. 11-0232. The theoretical densities of all compositions were calculated on the assumption that formation of α-Al_2O_3 is complete and zirconia is present in tetragonal form. The first assumption is justified on the basis of results of X-ray diffractions of sintered samples, presented later. The sinterability of composites is gradually increasing with HAp addition and these observations were made on the basis of bulk densities of the samples. It is very clear that the HAp additions in ZTA composites increasing the sinterability. The same may be predicted on the addition of fluoride compounds as magnesium and calcium fluoride because densification is observed more than pure ZTA composites sintered at the same temperature. The results of densities and other mechanical properties are given in Table 2.

The effects of second phases on the mechanical properties of ZTA can be observed in this table. The compressive strength and bending strength of the pure ZTA are about 470 MPa and 296 MPa respectively. When 10 wt% HAp was added under the same condition, the bending strength increased around 18 MPa, while the increase in compressive strength was 26 MPa. This

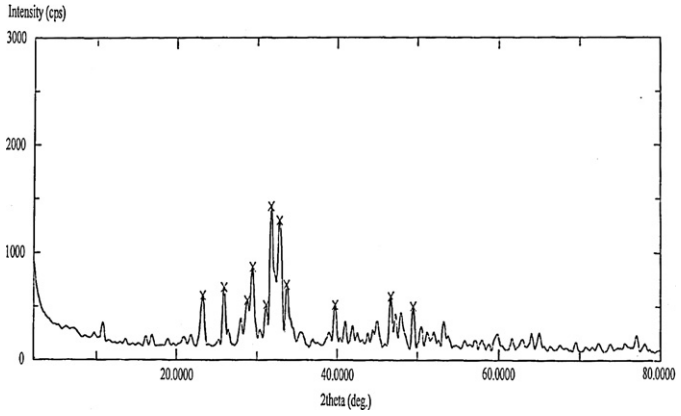

Fig. 2. XRD pattern of HAp powder, calcined at 1200 °C for three hours (marked peaks in the curve are of $Ca_4P_2O_9$; JCPDS file No. 11-0232).

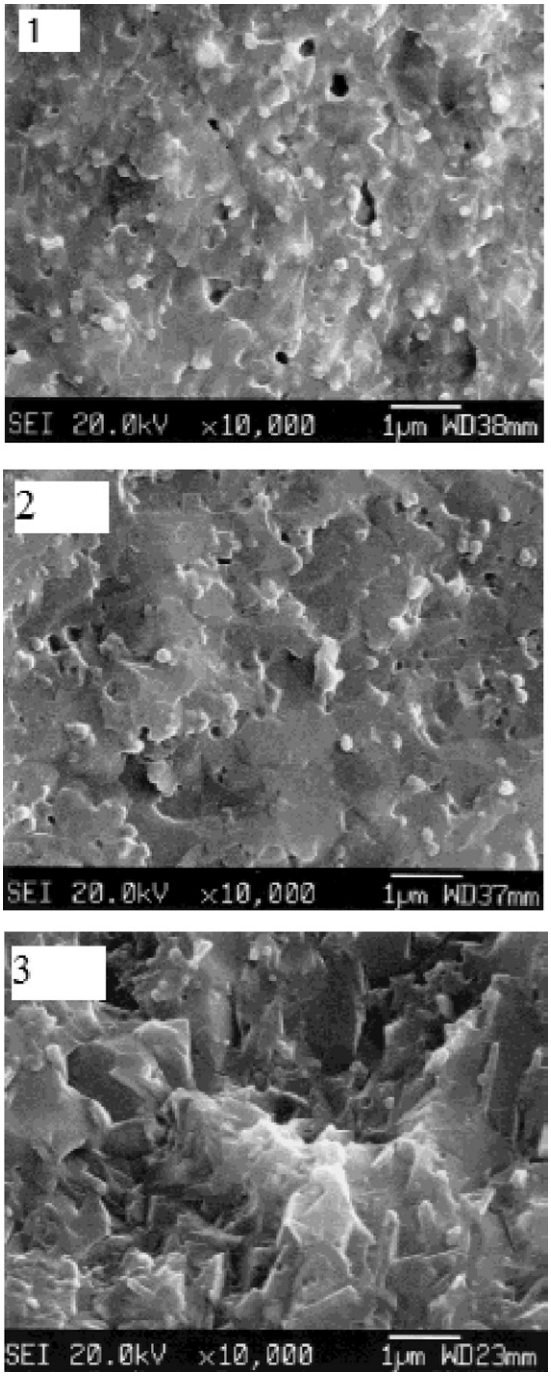

Fig. 3. SEM micrographs of fractured surface of sintered pellets having compositions (a) ZTA with 10 parts HAp, (b) ZTA with 20 parts HAp and (c) ZTA with 30 parts HAp.

improvement is believed to be closely related to better densification of ZTA in the presence of the HAp phase and fluoride compounds. This effectiveness is further increased by increasing the above contents.

In this study, it was observed that use of HAp powders and fluoride compounds as additives to ZTA are beneficial for improving mechanical properties. Lastly, in order to obtain optimal bio-mechanical property of the HAp added ZTA composites, the flexural strength and compressive strength should increase with increasing HAp content in the composites, and also presence of fluoride content, the strength is increasing. Therefore, there is a wide range of compositions that can be utilized for actual load-bearing biomedical applications. If the bioactivity is more important, up to 30% HA should be added to the composite. In this case, the strength of the samples of composites is higher than that of pure ZTA, while the bioactivity is another advantage. Strong ZTA composites can be fabricated with the addition of bioactive HAp for the purpose of improving their biocompatibility. Sintering of composites resulted in the formation of calcium phosphate phase ($Ca_4P_2O_9$) within the composites. The resultant body has high mechanical strength, while maintaining the excellent biocompatibility as discussed further.

SEM micrographs of the fracture surface of selected samples containing different types of second phase are shown in Fig. 3. Microstructures are dense and showing better sintering even at low temperature such as 1400 °C. When 10 and 20 parts of HAp are added in ZTA, the second phase is clearly distinguished and also its uniformity is maintained. In the case of composites, having 30 parts of HAp, it looks that extensive grain growth took place and the fracture surface occurred mostly in a transgranular pattern as shown in Fig. 3(c). The fracture surfaces become very rough and second phase is less clearly visible. It may be due to reactions between the calcium phosphate and alumina.

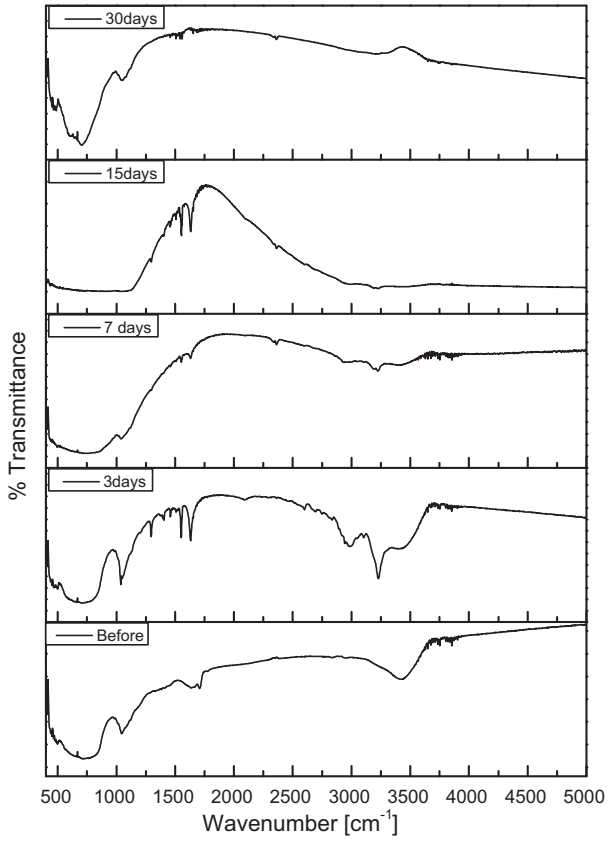

Fig. 4. FTIR spectra of ZTA composites samples containing 10 parts of HAp immersed in SBF solutions for different periods.

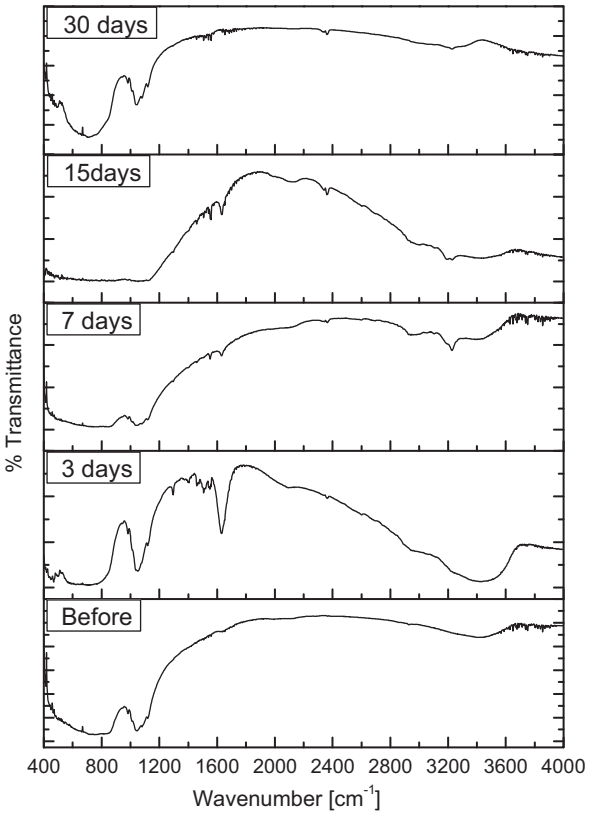

Fig. 5. FTIR spectra of ZTA composites samples containing 20 parts of HAp immersed in SBF solutions for different periods.

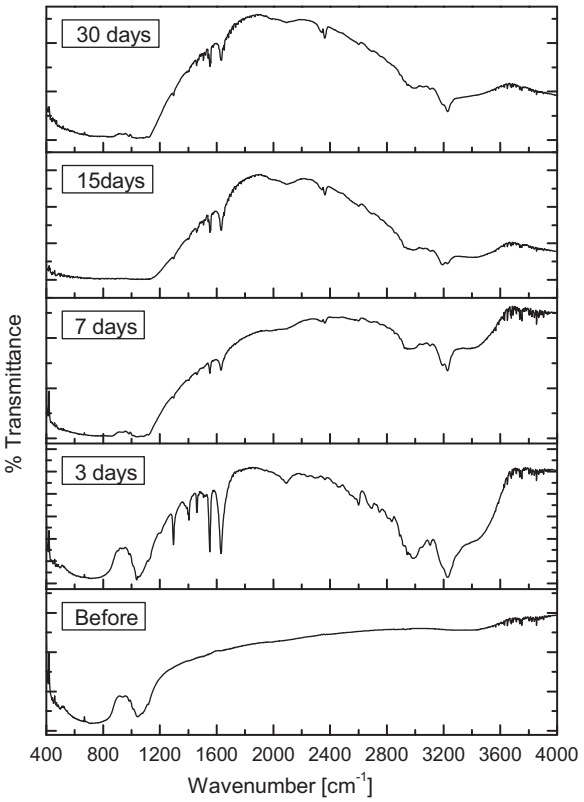

Fig. 6. FTIR spectra of ZTA composites samples containing 30 parts of HAp immersed in SBF solutions for different periods.

3.2. In vitro bioactivity in samples

The pH value of the SBF solution is changing towards basic and this confirms that the basic materials are being formed during SBF treatment given to HAp and fluoride doped ZTA composites. This observation confirms the formation of calcium and phosphate phases. The same changes were observed in all four composites. Starting pH value of SBF solutions was 7.2 in which samples were kept and then it was changing continuously and was observed around 8.2 on the 3rd day of soaking into SBF solution. Further it starts declining till the seventh date of treatment. This observation indicates the dissolution of calcium and the precipitation of phosphate on the surface of the sample. FTIR spectrum was used to determine the phases formed during SBF treatment. The FTIR bands confirm the development of phosphate and carbonated bands on the surface of the samples after soaking in SBF solution. This can be observed in Figs. 4–7, which are the results of FTIR. At wave lengths around 480, 680, 900, 1020 and 1550 (cm^{-1}), carbonate and phosphate bonds are appearing before SBF treatment in the samples of all composites. After 3 days, the new peaks have been developed after SBF treatment at wave number 1120,1300,1400,1430 and 1620 (cm^{-1}), which correspond to HCA. After 7 days, new O–H bonds were also observed. When samples were immersed for 15 days, mainly O–H and carbonate bonds were observed at the wave number 1520 and 1620 (cm^{-1}). The same results were also observed after one moth of soaking that peaks at 1520 and 1620 (cm^{-1}) were showing the

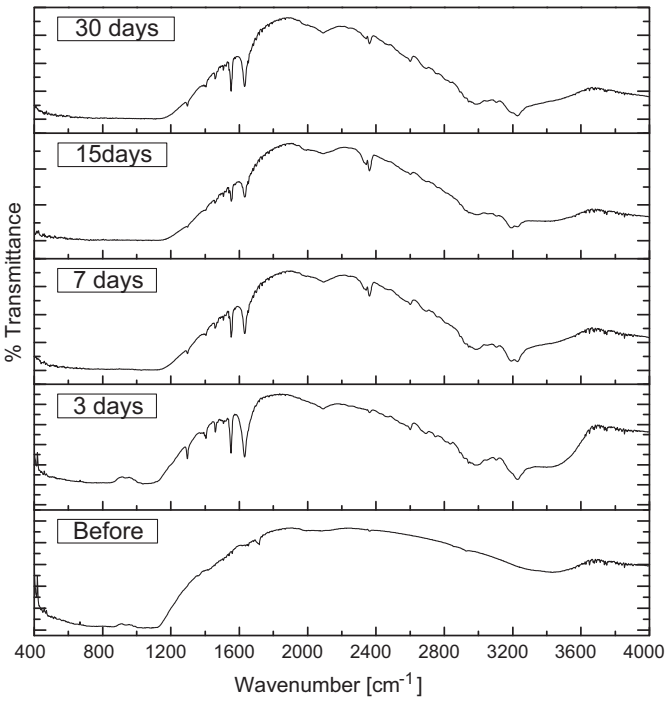

Fig. 7. FTIR spectra of ZTA composites samples containing 40 parts of HAp immersed in SBF solutions for different periods.

O–H and carbonate bonds. These bonds were continuously developing with the prolong SBF treatment. These results show that on the surfaces of the ZTA–HAp composites, the crystals are being deposited during SBF treatment. Thus, the deposited crystals are similar to bone-like apatite as confirmed by FTIR results. The crystal growth in SBF is attributed to the release of calcium ions due to the dissolution of calcium phosphate phase ($Ca_4P_2O_9$) present in ZTA–HAp composites and the bone-like apatite was deposited due to the formation of calcium phosphate clusters with the high concentration of calcium ions on the surface of samples. The deposition of apatite may occur in the pores of the composites if soaking period is increased. With increasing time, the surfaces of the ZTA–HAp composites can be covered with the bone-like apatite. Moreover, the bone-like apatite can be considered to enter the inside of the ZTA–HAp samples. The maximum formation of apatite occurred within 15 days. The immersion of SBF suggested that the ZTA–HAp composite had bioactivities. From these results it can also be observed that the bioactivity of composites of ZTA having 30 parts HAp is more than to the lower percentage as well as higher percentage of HAp in the composites.

4. Conclusions

Combined gel trapped precipitation process is beneficial for synthesis of fine powders. The nano size gel particles have pores in the same size range. Therefore, size of the material trapped in the pores is of the same order as of gel's particles. The process was used for preparing Al_2O_3–ZrO_2 composites and these powders showed better homogeneity and thermal reactivity. Uniaxially pressed samples showed higher sinterability with increasing percentage of HAp and introducing fluoride compounds. The compressive strength and fracture strength of all composites are also increasing with increasing content of HAp. The pH value of the SBF solutions remained high (∼8.2) up to the third day of soaking and further it declined. This observation indicates the dissolution of calcium and the precipitation of phosphate on the surface of the sample. The FTIR bands show that the development of phosphate and carbonated bands on the surface of the samples after soaking in SBF solution. The composites are showing bioactivity and it can also be concluded that the more bioactivity was observed with 30 parts HAp in the ZTA composites compared to the lower percentage as well as higher percentage of HAp in ZTA composites.

References

[1] L.M. Braun, S.J. Benninson, B.R. Lawn, Objective evaluation of short-crack toughness using indentation flaws: case study on alumina-based ceramics, J. Am. Ceram. Soc. 75 (1992) 3049–3057.

[2] P. Antoni, Tomsia, et al., Biomimetic bonelike composites and novel bioactive glass coatings, Eng. Mater. 7 (2005) 11.

[3] C. Correa, et al., Mechanical properties of alumina–zirconia composites for ceramic abutments, Mater. Res. 7 (4) (2004) 643–649.

[4] C. Piconi, G. Maccauro, Review: zirconia as a ceramic biomaterial, Biomaterials 20 (1999) 1–25.

[5] K. Tanaka, J. Tamura, K. Kawanabe, M. Nawa, M. Uchida, T. Kokubo, et al., Phase stability after aging and its influence on Pin-on-disk wear properties of Ce–TZP/Al_2O_3 nano composite and conventional Y–TZP, J. Biomed. Mater. Res. 67A (2003) 200–207.

[6] M. Ruhle, A.H. Heuer, Phase Transformation in ZrO2-Containing Ceramics II. The Martensitic Reaction in t-ZrO2, Advances in Ceramics. Science and Technology of Zirconia, American Ceramics Society, Columbus, 1984, pp. 14–32.

[7] M.N. Rahaman, et al., Ceramic for prosthetic hip and knee joint replacement, J. Am. Ceram. Soc. 90 (7) (2007) 1965–1988.

[8] D.J. Kim, M.H. Lee, D.Y. Lee, J.S. Han, Mechanical properties, phase stability, and bio-compatibility of (Y, Nb)-TZP/Al_2O_3 composite abutments for dental implants, J. Biomed. Mater. Res. (Appl. Biomater.) 53 (2000) 438–443.

[9] Y.-M. Kong, C.-J. Bae, S.-H. Lee, H.-W. Kim, H.-E. Kim, Improvement in biocompatibility of ZrO2–Al2O3 nano-composite by addition of HA, Biomaterials 26 (2005) 509–517.

[10] H. Moussa, et al., Bioactivity of sol–gel bioactive glass coated alumina implants, J. Biomed. Mater. Res. 52 (2000) 422–429.

[11] J.F. Shackelford, W. Alexander, Materials Science and Engineering Handbook, 3rd ed., Boca Raton, 2001, p. 461.

[12] W. Suchanek, M. Yashima, M. Kakihana, M. Yashima, Hydroxyapatite ceramics with selected sintering additives, Biomaterials 18 (1997) 923–933.

[13] P. Ducheyne, M. Marcolongo, E. Schepers, Bioceramic composites, in: L.L. Hench, J. Wilson (Eds.), An Introduction to Bioceramics, World Scientific Publishing Co., Singapore, 1993, pp. 281–297.

[14] J.W. Choi, Y.M. Kong, H.E. Kim, I.S. Lee, Reinforcement of hydroxyapatite bioceramic by addition of Ni_3Al and Al_2O_3, J. Am. Ceram. Soc. 81 (7) (1998) 1743–1748.

[15] Y.M. Kong, D.H. Kim, H.E. Kim, S.J. Heo, J.Y. Koak, Hydroxyapatite based composite for dental implants: an in vivo removal torque experiment, J. Biomed. Mater. Res. 63 (2002) 714–721.

[16] T.V. Thamaraiselvi, S. Rajeswari, Biological evaluation of bioceramic materials—a review, Trends Biomater. Artif. Organs 18 (1) (2004) 9–17.

[17] J. Li, L. Hermansson, R. Söremark, High strength biofunctional zirconia: mechanical properties and static fatigue behavior of zirconia–apatite composites, J. Mater. Sci. Mater. Med. 4 (1993) 50–54.

[18] S. Deville, et al., Influence of surface finish and residual stresses on the ageing sensitivity of biomedical grade zirconia, Biomaterials 27 (2006) 2186–2192.

[19] E. Adolfsson, P. Alberiushenning, L. Hermansson, Phase-analysis and thermal-stability of hot isostatically pressed zirconia–hydroxyapatite composites, J. Am. Ceram. Soc. 83 (2000) 2798–2802.

[20] A. Rapacz-Kmita, A. Slosarczyk, Z. Paszkiewicz, Mechanical properties of HAp–ZrO_2 composites, J. Eur. Ceram. Soc. 26 (2006) 1481–1488.

[21] L. Gremillard, et al., Durability of zirconia-based ceramics and composites for total hip replacement, in: G. Daculsi, P. Layrolle (Eds.), 20th International Symposium on Ceramics in Medicine, 2007, 791–794.

[22] J. Chevalier, What future for zirconia as a biomaterial, Biomaterials 27 (2006) 535–543.

[23] R. Lenk, State of the art in ceramic manufacturing, in: J.A. D'Antonio, M. Dietrich (Eds.), Ceramic and Orthopaedics: 10th BIOLOGIX Symposium Proceedings, 2005, pp. 175–179.

[24] V.V. Silva, F.S. Lameiras, R.Z. Dominguez, Microstructural and mechanical study of zirconia–hydroxyapatite (ZH) composite ceramics for biomedical applications, Compos. Sci. Technol. 61 (2001) 301–310.

[25] W. Pyda, A. Sl osarczyk, Z. Paszkiewicz, A. Rapacz-Kmita, M. Haberko, A. Pyda, Polycrystalline hydroxyapatite material reinforced with zirconia inclusions, Composites 1–2 (2001) 133–136.

[26] R.B. Heimann, T.A. Vu, Effect of CaO on thermal decomposition during sintering of composite hydroxyapatite–zirconia mixtures for monolithic ceramic implants, J. Mater. Sci. Lett. 16 (1997) 437–439.

[27] A. Krajewski, A. Ravaglioli, N. Roveri, A. Bigi, E. Foresi, Effect of fluoride, chloride and carbonate ions introduced by cyclic pH fluctuation on the physico-chemical properties of apatite-based ceramics, J. Mater. Sci. 25 (1990) 3203–3207.

[28] E.C. Moreno, M. Kresak, R.T. Zahradnik, Fluoridated hydroxyapatite solubility and caries formation, Nature 274 (1974) 64–65.

[29] R.Z. Legeros, L.M. Silverstone, G. Daculsi, L.M. Kerebel, In vitro caries-like lesion formation in F-containing tooth enamel, J. Dent. Res. 62 (1985) 138–144.
[30] G.S. Ingram, P.F. Nash, Mechanism for the anticaries action of fluoride, Caries Res. 14 (1980) 298–303.
[31] E.J. Duff, A.A. Grant, Apatite Ceramics for Use in Implantation, Advances in Biomaterials. Mechanical Properties of Biomaterials, vol. 2, Wiley, New York, 1980, pp. 465–475.
[32] F.B. Ayed, J. Bouaziz, K. Bouzouita, Pressureless sintering of fluorapatite under oxygen atmosphere, J. Eur. Ceram. Soc. 20 (2000) 1069–1076.
[33] W. Rajarao, R.F. Boehem, A study on sintered apatites, J. Dent. 53 (1974) 1351–1355.
[34] V.K. Singh, R.K. Sinha, Alumina by a combined precipitation and gelation process, Mater. Lett. 18 (1994) 201–206.
[35] V.K. Singh, R.K. Sinha, Low temperature synthesis of spinel ($MgAl_2O_4$), Mater. Lett. 31 (1997) 281–285.
[36] V.K. Singh, S. Singh, R-curve behaviour in nano crystalline spinel ($MgAl_2O_4$), Adv. Appl. Ceram. 22 (2) (2006) 1–3.
[37] V.K. Singh, Preparation of bio grade alpha alumina and its crack growth resistance behaviour, Trans. Indian Ceram. Soc. 66 (2) (2006) 85–88.
[38] V.K. Singh, K.S. Arun, K.C. Raj, Tetragonal ZrO_2 in alumina matrix from combined gelation–preciptation method, Indoceram 45 (2) (2008) 34–39.
[39] V.K. Singh, S. Abhinav, K. Vijay, S. Singh, Sintering studies of combined gelation–precipitation processed Al_2O_3–ZrO_2 nanocomposites, in: Technical Proceedings of National Symposium on "Ceramics: Energy and Environment", Organised by Indian Ceramic Society, Kolkata, India, 11–13 January 2011, (2011), pp. 204–208.
[40] V.K. Singh, Fracture behaviour of gel processed Al_2O_3–MgO–ZrO_2 composites, Ph.D Thesis, Department of Ceramic Engineering, IT-BHU, 1993.
[41] V.K. Singh, R.K. Sinha, Combined gel-precipitation process for multi-component ceramics, in: Proceedings of Indian Ceramic Society, 1996, pp. 197–201.
[42] I. Mobasherpour, M. Solati Hashjin, S.S. Razavi Toosi, R. Darvishi Kamachali, Effect of the addition ZrO_2–Al_2O_3 on nanocrystalline hydroxyapatite bending strength and fracture toughness, Ceram. Int. 35 (2009) 1569–1574.
[43] M. Razavi, M.H. Fathi, M. Meratian, Fabrication and characterization of magnesium—fluorapatite nanocomposite for biomedical applications, Mater. Charact. 61 (2010) 1363–1370.
[44] L.A. Yuan, A. Li-Yu Jin, M.W. Julian, C.D. Quinn, A. Paul, E. Komesaroff, A new sol–gel process for producing Na_2O-containing bioactive glass ceramics, Acta Biomater. 6 (2010) 4143–4153.
[45] M. Ferraris, E.H. Verne, P. Appendino, C. Moisescu, A. Krajewski, A. Ravaglioli, A. Piancastelli, Coatings on zirconia for medical applications, Biomaterials 21 (2000) 765–773.
[46] J.J. Blakera, S.N. Nazhatb, A.R. Boccaccinia, Development and characterisation of silver-doped bioactive glasscoated sutures for tissue engineering and wound healing applications, Biomaterials 25 (2004) 1319–1329.
[47] A.U.J. Yap, Y.S. Pek, R.A. Kumar, P. Cheang, K.A. Khor, Experimental studies on a new bioactive material: haionomer cements, Biomaterials 3 (3) (2002) 955–962.
[48] Y.W. Gua, A.U.J. Yapb, P. Cheanga, K.A. Khorc, Effects of incorporation of HA/ZrO_2 into glass ionomer cement (GIC), Biomaterials 26 (2005) 713–720.
[49] W. Jian, H. Chunpeng, W. Qianbing, C. Yifan, C. Yonglie, Characterization of fluoridated hydroxyapatite/zirconia nano-composite coating deposited by a modified electrocodeposition technique, Surf. Coat. Technol. 204 (2010) 2576–2582.
[50] Laminated and functionally graded hydroxyapatite/yttria stabilized tetragonal zirconia composites fabricated by spark plasma sintering, Biomaterials 24 (2003) 667–675.
[51] G. Hongbo, A.K Khiam, C.B. Yin, M. Xigeng, Alkaline phosphatase grafting on bioactive glasses and glass ceramics, Acta Biomater. 6 (2010) 229–240.
[52] T. Kokubo, H. Kushitani, S. Sakka, T. Kitsugi, T. Yamamuro, Solutions able to reproduce in vivo surface-structure changes in bioactive glass-ceramic A-W, J. Biomed. Mater. Res. 24 (1990) 721–734.
[53] T. Kokubo, H. Takadama, How useful is SBF in predicting in vivo bone bioactivity, Biomaterials 27 (2006) 2907–2915.